PRESENT LIMITS OF OPERATION OF PRODUCT LUBRICATED AND MAGNETIC BEARINGS IN PUMPS

by

Michael K. Swann

Vice President and General Manager

Glacier RPB Inc.

Mystic, Connecticut

Jonathan Watkins

Product Manager, Ceramic Bearings

The Glacier Metal Co. Ltd.

Middlesex, United Kingdom

and

Kevin R. Bornstein

Senior Engineer, Magnetic Bearings

Glacier RPB Inc.

Mystic, Connecticut

Michael K. Swann is Vice President and General Manager of Glacier RPB Inc. of Mystic, Connecticut, the North American subsidiary of Glacier RPB. Glacier RPB Inc. performs application engineering of fluid film bearings and detailed design, engineering and manufacturing of magnetic bearing systems for turbomachinery. Mr. Swann was formerly with Magnetic Bearings, Inc. He has also held positions in the power and process industries with Proto-Power Corporation and Union Carbide Corporation, respectively. Mr. Swann received his B.S. (Mechanical Engineering) from the University of Connecticut and his M.S. (Mechanical Engineering) from Northeastern University. He is a registered Professional Engineer in the State of New York.

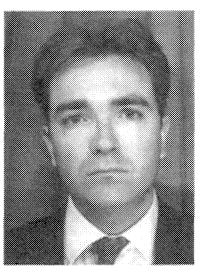

Jonathan Watkins is Product Manager, Ceramic Bearings, for Glacier RPB in Northwood Hills, Middlesex, England. Mr. Watkins received his B.S. (Materials Science and Technology) from the University of Birmingham, UK, and a postgraduate certificate in design, manufacture and management from the University of Cambridge, UK. Before his present role, he spent over three years in the Manufacturing Technology Task Force of T&N plc. He has also worked on carbon fiber composites research for ICI plc.

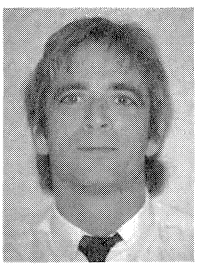

Kevin R. Bornstein is a Senior Engineer with Glacier RPB Inc., of Mystic Connecticut, the North American subsidiary of Glacier RPB. Mr. Bornstein was formerly with Magnetic Bearings, Inc., and has extensive experience in the design and commissioning of magnetic bearing systems throughout North America and Europe including several pumps. Mr. Bornstein received his B.S. (Physics) from the University of Connecticut.

ABSTRACT

Interest in nonoil lubricated bearings is growing, due to a number of benefits derived from these bearings: improved pump performance and reliability, enhanced pump maintainability, elimination of the cost and maintenance of separate systems for lubrication oil and shaft seals, reduction in pump size and weight, reduced power consumption, elimination of oil disposal costs, elimination of potential for product contamination, and elimination of leakage of a hazardous fluid to the environment.

This trend has allowed two types of nonoil lubricated bearings to grow in favor: 1) bearings lubricated by the process media and 2) magnetic bearings.

The state-of-the-art in these different technologies, as applied to pumps, is examined to identify what the current limits in the application of these technologies are. In the case of product lubricated bearings, the present mechanical limits, film thickness, and temperature limits, as related to different material and lubricant combinations, are reviewed by reference to bearing theory of operation and actual pump application. The role of

various lubricant and material properties and mechanical design features are reviewed for these types of bearings. In addition, the importance of proper lubricant circulation and filtering is highlighted. The relationship of the above design parameters to specific load, speed, and temperature is examined to produce limiting operating envelopes for these types of bearings, similar to that previously developed for oil lubricated tilting pad bearings.

Magnetic bearing applications completely circumvent the dry running and contamination issues raised by product lubricated bearings and offer unmatched capabilities in pump diagnostics. Space envelope and cost are usually not as favorable as product lubricated bearings. Limitations in operation of magnetic bearings are related to specific load, frequency, temperature, and system stability. The development of limiting envelopes of operation for magnetic bearings is presented to allow pump designers and end users to assess bearing load capacity *vs* frequency characteristics. Control of rotor and stator natural frequencies often demands special attention in any given application. In certain submerged bearing applications, corrosion considerations represent the most restrictive limitation in the application of magnetic bearings. In theory, almost any type of process fluid may be handled with magnetic bearings, and a growing variety of applications have already been successful.

INTRODUCTION

Bearings for rotating machinery are usually rated in terms of a design load capacity, speed capability, and ambient temperature and environmental capability. Leopard [1] identified the limits in operation for oil lubricated tilt pad thrust and journal bearings. He showed how the classic limits of film thickness, pad temperature, oil oxidation, and mechanical limits due to stress can be defined for a given bearing and used by machine designers and operators to assess the limiting envelope for safe operation. The limits discussed were derived from both theoretical and empirical considerations. The specific design issues of pad surface material; pad design; lubricant type, quantity, temperature, pressure, and system type; bearing alignment, dirt and filtration and clearance were examined to show how these contribute to the determination of the three fundamental limits of film thickness limit, mechanical limit, and temperature limit.

There are, of course, other bearing considerations in the quest for high performance, reliable machines. Most notable of these are stiffness and damping characteristics. In order to realize acceptable rotordynamic response, the bearing stiffness and damping properties must be optimized to allow machine operation throughout the entire bearing safe operating regime; operation that might be "safe" for the bearing is not necessarily "safe" for the rest of the machine. Seal life may be adversely affected. Shaft failures due to vibration fatigue may develop. The Leopard [1] approach may be employed in the definition of limiting envelopes for safe operation of product lubricated bearings and active magnetic bearings for pump applications. Thus, once developed and assuming rotor bearing stability, the safe operating regimes could be employed to show that the bearing would serve its function for a very long time.

There are strong incentives that are driving machine manufacturers and end users to consider these alternative bearing technologies. Heretofore, pump designers have seen slow evolutionary changes in the mechanical technologies they employ. Bearing technology, as applied to pumps, has not fundamentally changed since the introduction of the tilt pad bearing more than 30 years ago. Hydrodynamic or rolling element bearings employing oil lubrication have been utilized requiring separate lubrication systems and shaft sealing systems for the bearings. In certain small pump applications, plain bushings and thrust washers have been successfully employed with product lubrication.

As explained by Smith [2], the retirement of oil lubrication technology eliminates the lubrication system and bearing seals and associated costs, and also provides the opportunity for a small revolution in pump design. Mechanical seals can be totally eliminated for canned motor and magnetic drive pumps. Further cost savings become possible as the bearings are moved from outside the pump housing to inside. The shaft becomes shorter and the pump housing may become simpler leading to higher reliability and reduced maintenance costs. Significant overall size and weight savings become possible making these bearings especially attractive in offshore application. Examples of the simplicity realized in actual pump application of product lubricated bearings and magnetic bearings are shown in Figures 1 and 2, respectively.

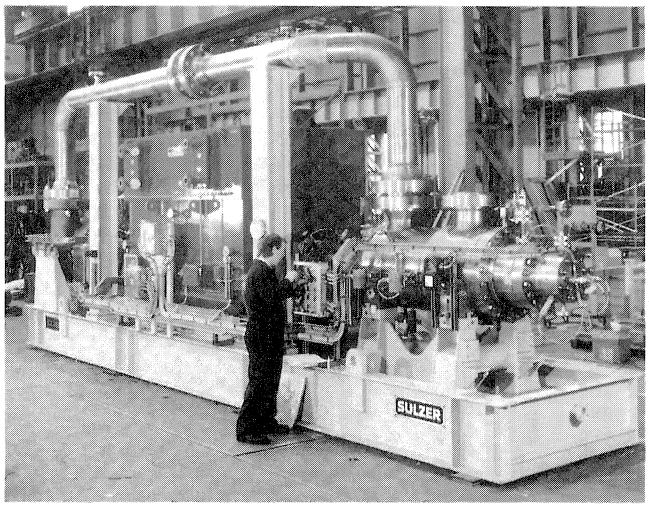

Figure 1. Sea Water Injection Pump with Ceramic Tilting Pad Radial and Axial Bearings.

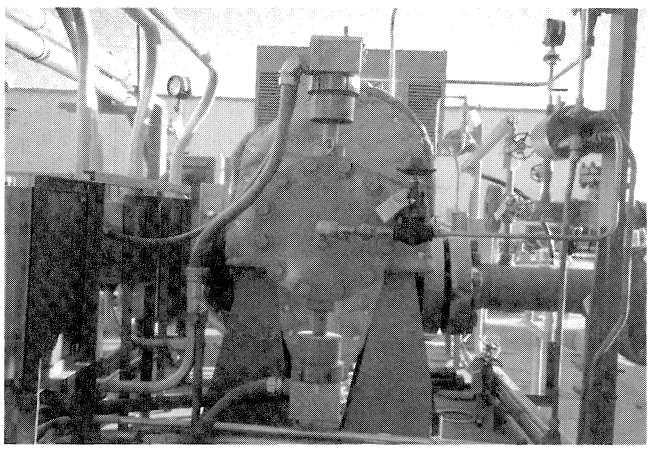

Figure 2. Boiler Feedwater Pump with Canned Magnetic Radial Bearing System.

Both product lubricated bearings and magnetic bearings have significant power savings when compared to oil lubricated bearings. The complete elimination of oil shear, oil churning losses, and pumping losses with a magnetic bearing makes this option especially attractive for significant mechanical efficiency increases. The product lubricated bearing also offers reduced power consumption, since the viscosity of most common pumped fluids is substantially lower than oil.

Most significantly, both bearing types also provide the opportunity to reduce or eliminate fugitive emissions, especially

where the driver is also sealed from the environment. Also, elimination of oil prevents the possibility of oil contamination of product and there is no need to replace and dispose of lubricating oil. Lastly, elimination of oil reduces the risk of fire.

Marscher and Jen [3], identified the types of centrifugal pumps for which there is a current need for advanced bearing technologies. These include: 1) pumps in which leaks are intolerable due to environmental or safety hazards, including many chemical pumps and any application where canned motor pumps are considered, 2) pumps installed in relatively inaccessible areas or in services where long maintenance intervals could be an economic advantage such as certain pumps in nuclear service, 3) pumps where contamination of the bearing lubricant contributes to premature bearing failure, and 4) relatively high speed pumps, such as boiler feed pumps and aerospace fuel pumps that have often suffered from rotordynamic difficulties, particularly at low load.

PRODUCT LUBRICATED BEARINGS

Introduction to Product Lubricated Bearings

Product lubricated bearings differ from traditional oil lubricated bearings, because they use the process liquid or pumped fluid (for example, sea water, hydrocarbons, crude oil) as the lubricant. Although such process lubricants do not have the same hydrodynamic characteristics as oils, they are sufficient for bearing materials that possess the correct load bearing and surface properties. The bearing design must consider the fluid properties. Product lubricated bearing design is based on current oil lubricated bearing practice modified to take into account changes in specific heat, viscosity, density, and thermal conductivity of the lubricant. Also, the bearing failure criteria have been altered. Product lubricated bearings for high load and/or high temperature service are currently made from either ceramic or polymer coated steel depending upon the particular application. Early stainless steel pad designs running against graphite mating surfaces have also met with some success, but are not very wear resistant.

Polymers in general, and thermoplastics specifically, possess excellent surface properties compared to metallic materials. In particular, they show good compatibility (seizure resistance) and conformity when run against conventional steel counterfaces. These attributes make this class of materials attractive bearing materials. However, because of their lack of mechanical strength and their poor thermal properties, polymers are used in the form of a thin layer bonded to a steel backing for most bearing applications. One of the most successful materials to date has been a compound based on polyetheretherketone (PEEK) with PTFE and graphite fillers. It is normally bonded by a porous bronze sinter layer to steel backing and is compatible with most pump liquids. The design allows operation from −150°C to 250°C. Examples of PEEK tilting pad thrust and journal bearings are shown in Figures 3 and 4, respectively.

Ceramic properties are significantly different from those of polymers and metallic bearing alloys. These properties offer new technical possibilities in the design of pump bearing systems, particularly in harsh operating conditions. Ceramic bearings are used for applications where the process fluids are of low viscosity, contaminated, and operating at temperatures too high or too low for even PEEK type materials. Ceramics are ideally suited to such conditions because of their extreme hardness, high compressive strength, extreme temperature capability, and seizure resistance capability. A number of materials have been tested for product lubricated bearings but by far the most appropriate material to date has been monolithic silicon carbide, a material with hardness twice that of tungsten carbide.

Silicon carbide thrust and journal bearing assemblies, respectively, are shown in Figures 5 and 6. As in the case of oil lubricated tilt pad bearings, combined journal and thrust

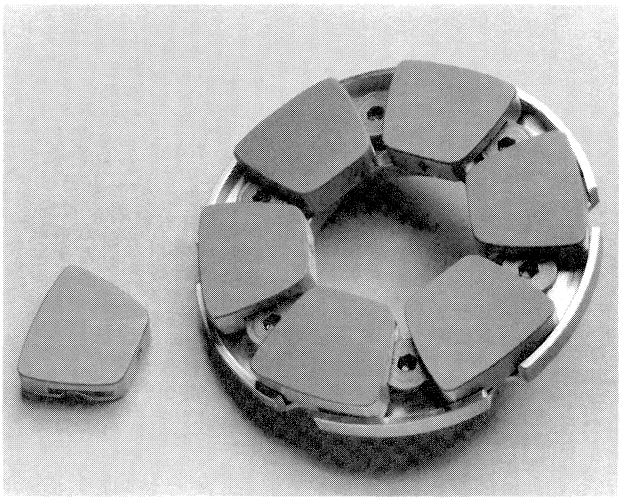

Figure 3. PEEK Tilting Pad Axial Bearing.

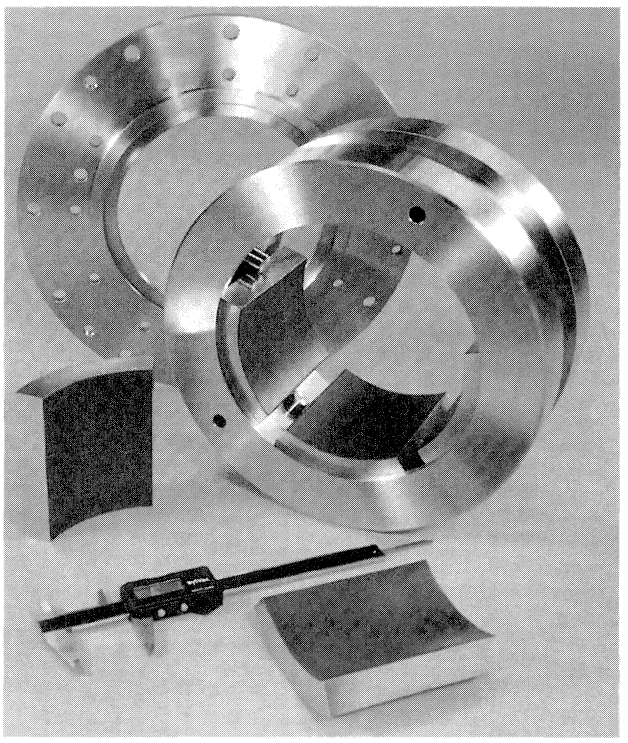

Figure 4. PEEK Tilting Pad Radial Bearing.

assemblies are possible (Figure 7). Note the requirement for mating running surfaces of the same, or similar, ceramic material.

Why Tilting Pad Product Lubricated Bearings

For small bearing applications, low cost plain bushings and grooved thrust washers often offer a viable solution to meet the needs of the pump. However, for larger bearings, the cost disadvantage of tilting pad bearings becomes smaller compared to plain bushings and thrust washers. More importantly, the advantages of tilting pad bearings far outweigh the cost differential:

- The ability to accommodate misalignment. This is particularly important with low viscosity lubricants such as sea water, which produce very small films.

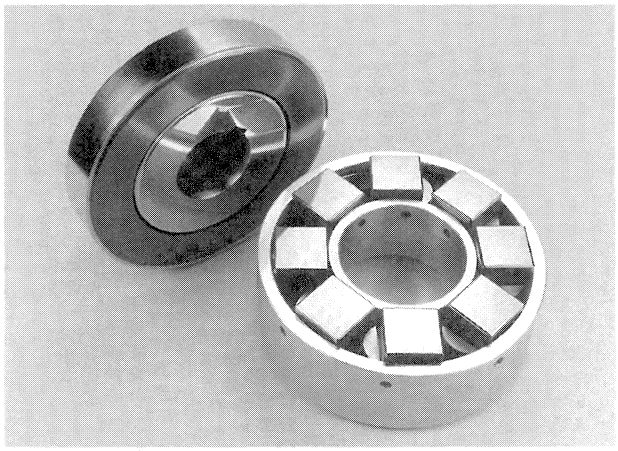

Figure 5. Silicon Carbide Tilting Pad Axial Bearing.

Figure 6. Silicon Carbide Tilting Pad Radial Bearing.

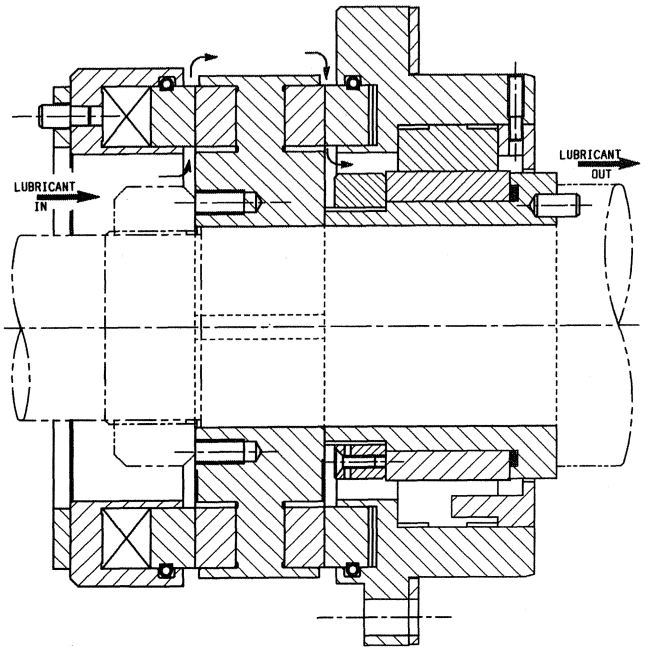

Figure 7. Combined Silicon Carbide Tilting Pad Axial and Radial Bearing Assembly.

- The ease of lubrication made possible by the gaps between the pads. Plain bushings require significant differential pressure across the bearing or costly machining of axial grooves in the bearing bore.
- Better stability characteristics than cylindrical bore bushings.
- Plain bushings require a tight fit in the housing that has to be maintained throughout the operating temperature range. This fit can cause problems at assembly or dismantling of the bearing.
- Tilting pad bearings have good startup conformity.

How Old and New Tilt Pad Design Features Accommodate the Change to Product Lubrication

The design of the PEEK bearings is essentially the same as those made from white metal; the polymeric coating enables the option of product lubrication. The steel backing provides the underlying strength, while the bronze interlayer provides both a strong mechanical bond for the polymer lining and dimensional stability.

However, the traditional white metal tilting pad design has been changed for ease of manufacture for ceramic bearings to take into account the extremely thin hydrodynamic films and to minimize stress raisers that could precipitate brittle fracture. Therefore, the design of the tilting pads has been kept as simple as possible avoiding large changes of cross section, sharp corners, or undercuts. The resultant thrust pad design is one with offset pivots. The amount of offset is far more than comparable PEEK or white metal pads.

Methods of Overcoming Misalignment and Temperature Differentials (Ceramic)

Ceramic sleeves are a limitation in the use of ceramic radial bearings. To overcome misalignment and temperature differentials, a range of sleeve designs has been developed that may also incorporate inconel tolerance rings, as shown in Figure 8. This type of sleeve allows greater operating temperature ranges and gives some degree of alignment capability. In addition, the O-rings in the sleeve assemblies allow axial thermal expansion. In some cases, low expansion alloys can be substituted for standard materials (duplex and stainless steels) to reduce thermal expansion problems.

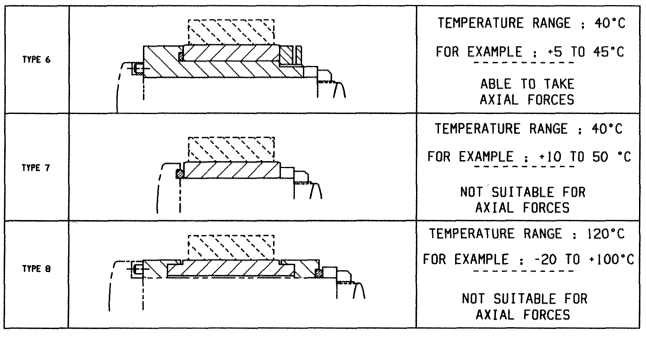

Figure 8. Silicon Carbide Radial Bearing Sleeve Types.

General Design and Environmental Limits of Operation of Tilt Pad Bearings

For a given size tilting pad bearing under given lubricant conditions, Martin [4] has shown how a limiting envelope can be produced for safe operating load *vs* sliding speed. This limiting envelope is defined by three different conditions shown in Figure 9:

- Film thickness limit (low speed operation)
- Mechanical limit (medium speed operation)
- Temperature limit (high speed operation)

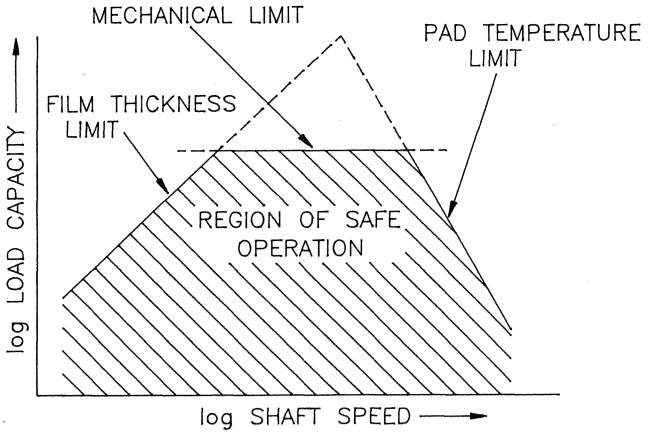

Figure 9. Limiting Operating Envelope for Tilting Pad Bearings.

It is possible to rationalize some of the variables that affect full hydrodynamic operation and combine them with practical experience to produce curves of acceptable minimum film thickness for various bearing sizes. Such curves have been derived by Martin [4], for tilting pad bearings and are of the form:

$$Wp = \frac{\eta_e b L^2}{Ch^2_{min}} U \qquad (1)$$

These curves can be plotted as the positively sloping curve defining the low speed boundary in Figure 9.

This basic film thickness limit is not very constraining for oil lubrication, but becomes a real restriction on low viscosity fluids used for product lubrication as seen by the h^2_{min} term in Equation (1).

For slow speed bearings, the film thickness limit can be altered if a pad surface material is used that will withstand short periods of boundary lubrication with negligible wear. Clearly, this is no longer hydrodynamic lubrication, but for this type of operation it is usual to rate bearings by hydrodynamic theory using a smaller limiting film thickness to allow for the different pad surface material.

The temperature limit for a given bearing is dependent on the characteristics of the surface material. This limit usually forms a right side boundary to the limiting envelope of operation in Figure 9 and represents the load and speed combinations at which sufficient heat is generated within the film to damage the bearing material.

The peak of the envelope formed by the film thickness limit and the temperature limit is truncated by the mechanical limit. The design features that limit the pad design to a specific load are:

- *Pad thickness*–For optimum operation the pad should crown slightly and this crowning is achieved by a combination of thermal effects, initial machining, and deflection due to load. A pad that is too thin, relative to the load, will result in excessive crowning.
- *Pivot area*–Stresses at the pad pivot are high and can exceed the elastic limit of the pad material. Under dynamic conditions, fretting can occur in this area if the load is too high. The pivot area cannot be increased without losing bearing performance (restricting pad tilt).

It is convenient to plot the limiting operating envelope on log-log paper, since the thin film limit and the mechanical limit will appear as straight lines defining two of the envelope boundaries. In many cases, the temperature limit of the bearing material may also be plotted as a simple line. Note that one such plot would be required for each inlet lubricant temperature and environmental temperature condition for a specific bearing.

Design and Environmental Limits of Operation of Product Lubricated Bearings

Film Thickness Limit

The viscosities of most pumped fluids of interest are lower than that of oil, meaning that the film thickness boundary of the limiting envelope of operation will move to the right eliminating certain load and speed combinations that would be acceptable for oil lubrication. For example, the change in the operating envelope is displayed in Figure 10 by Leopard [5], when changing from oil lubrication to water lubrication for a given bearing.

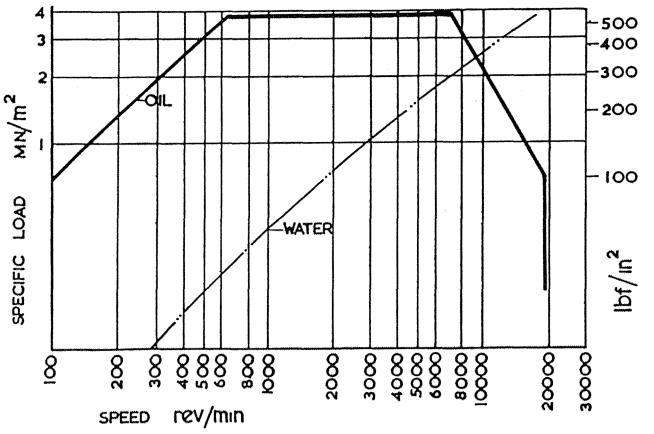

Figure 10. Comparison of Load Capacity of Tilting Pad Thrust Bearing with Oil and Water Lubrication.

The reduction in the film thickness limit can be exacerbated by variations in the operating temperature environment and the process fluid temperature due to the attendant viscosity changes. However, these circumstances do not inhibit the many successful applications that have been made. This problem is often mitigated by the close control of surface finish of the finished bearing product, particularly in the case of silicon carbide.

Mechanical Limit

Tests have shown that PEEK bearings are able to operate with specific loads of over three times their normal design limit of 3.9 MPa (565 psig). Under dynamically loaded test conditions, the fatigue strength of PEEK has been found to be comparable with that of aluminum-tin plain bearing alloys. Fatigue of the bronze sinter interlayer occurs before damage to the PEEK polymer lining.

Ceramics, on the other hand, have even higher load bearing capabilities arising from their greater compressive strength. For example, a silicon carbide tilting pad axial bearing has been shown to be capable of carrying a specific loading of 32.5 MPa. Overloading failure is displayed as a catastrophic brittle failure of the ceramic. However, the normal design limit is 8.5 MPa (1230 psig) for a fully equalized thrust bearing.

Temperature

PEEK can withstand operating temperatures of −150°C to 250°C and up to 300°C for short periods (up to 120°C higher than white metal). As the temperature increases, the load bearing capacity of the PEEK pads decreases; tests have shown that the load capacity can be reduced by 50 percent when operating temperatures increase from 80°C to 240°C, as a result of reduced hydrodynamic film thickness.

When PEEK is used with high viscosity lubricants, shear action can cause large temperature rises at high sliding speeds because of

the poor surface thermal conductivity of the material. Also, tests have shown that the load capacity of PEEK reduces by approximately 50 percent if the lubricant temperature is increased from 70 to 240°C. Beyond the load limit, there is a "wiping" of the PEEK coating. Beyond 240°C, there is a rapid fall in load capacity.

Tests show that tilting pad ceramic bearings are easily capable of operating at sliding speeds ranging from 7 m/s (23 fps) to beyond 20.9 m/s (68 fps). Because of the low viscosity of the product lubricants and the high temperature capability of silicon carbide, the sliding speed is not usually a limitation. Accordingly, no right side boundary is normally shown in the envelope for safe operation of silicon carbide radial and axial bearings, Figures 11 and 12, respectively.

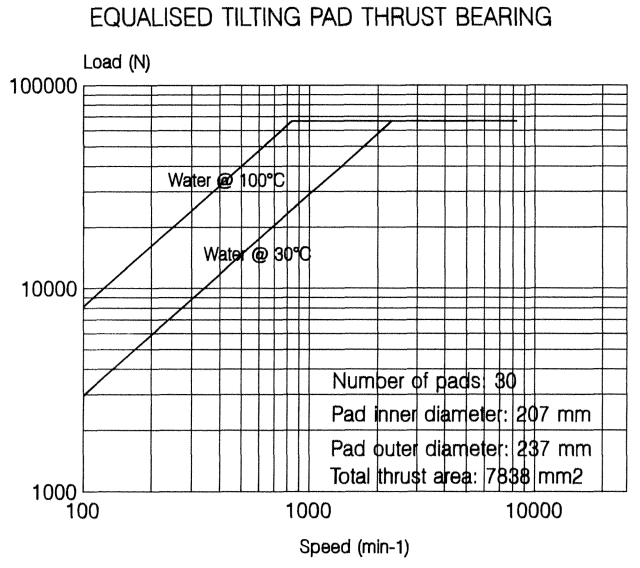

Figure 11. Typical Operating Envelope for Silicon Carbide Tilting Pad Axial Bearing.

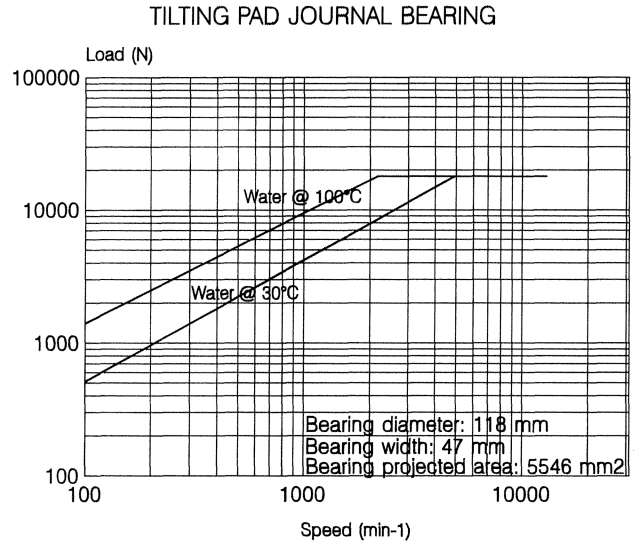

Figure 12. Typical Operating Envelope for Silicon Carbide Tilting Pad Radial Bearing.

Silicon carbide bearings are presently designed to operate between −200°C and 380°C, although the flash point of the lubricant and attendant dry running may preclude use at the higher temperatures if sufficient pressure is not available to prevent flashing.

Lubricant flash temperature may define a right side boundary to the limiting operating envelope. The lubricant flash temperature is highly dependent upon the material combination chosen for the moving and static surfaces. Also, the pressure and thermal properties of the lubricant are important. Low lubricant specific heat and low material thermal conductivity are detrimental to the flash temperature. Water has a major disadvantage as a lubricant because of its low boiling point and corresponding flash point. In a pump in which the pressure of the liquid can fluctuate widely, the highest lubricant temperature allowed must be based upon the lowest possible pressure in order to have a sufficient safety margin to prevent flashing.

A further complication may arise in the case of silicon carbide bearings due to differential thermal expansion. Because the thermal expansion coefficient of silicon carbide is much less than most steels, stressing or loosening of the ceramic parts may occur, particularly in the case of silicon carbide sleeves and thrust collars. Therefore, the combined operating and static temperature range may limit the ceramic bearing application unless careful design is undertaken to compensate for these effects. As previously discussed, special design features have been developed to overcome these difficulties.

Lubricant Corrosivity

Silicon carbide is extremely resistant to chemical attack. Only during dry running conditions can oxidation occur. In some cases, oxidation may be beneficial because of the smooth silica layer formed under these conditions.

Both sintered and reaction bonded silicon carbide are now being used in actual applications. For journal components, reaction bonded silicon carbide (RBSC) is commonly used; this comprises silicon carbide grains within a free silicon matrix, the surface of which is oxidized to silica. After processing, it comprises silicon carbide with two to three percent free silicon filling intergranular porosity and increasing its fracture toughness. Being acidic, the surface silica can be etched away by alkaline lubricants such as NaOH; tests have shown that the intergranular etching occurs with NaOH solution (pH 12) down to a maximum depth of 10 μm. Beyond this depth, there is no residual free silica to leach out, thus there is no overall degradation to the hydrodynamic load capacity. During the tests described, the silicon carbide grains remained intact and the test conditions had little or no effect on the mechanical properties of the bearing even after 5000 hours running.

For PEEK bearings, the corrosivity of the lubricant is only a factor when considering the backing material of the PEEK pads. PEEK itself is extremely inert and will resist attack from the vast majority of organic and inorganic liquids. PEEK is compatible with most lubricating oils up to 150°C and is resistant to oxidation products that may occur above 115°C.

Role of Lubricant Cleanliness

For tilting pad bearings in general, the lubricant should be filtered such that there are no dirt particles greater than the minimum film thickness present. For oil lubricated white metal bearings this means filtration down to 15 to 20 μm. With the thinner films that arise with product lubrication, contamination can be a problem in two ways: contaminants can disrupt the hydrodynamic film, and they can damage the bearing surfaces.

As an example, the design film thickness for PEEK coated bearings lubricated by water will have to be increased by the presence of dirt particles greater than 10 μm. This results in a larger bearing running at a lower load capacity than would occur in a clean environment. In addition, higher wear rates would be expected.

Ceramic, owing to its hardness (40,000 N/mm^2), can tolerate fine abrasive impurities in the lubricant that are much larger than the minimum film thickness (down to 1 μm). Therefore, filtering can often be avoided. Hard particles in the size range 50 to 200 μm often scratch the surface of the ceramic before being ground to fine dust in the zone of minimum fluid film thickness. During one extensive test program, crushed silica was injected into the pump (95 percent by weight–less than 25 μm in size, 40 percent by weight–more than five μm in size) to a concentration of 1000 ppm by weight in lubricant with no apparent effect on temperature rise, drive torque, or pad condition. Accordingly, contaminants have little effect on the normal mechanical load limit except where debris is sufficiently large to interfere with the tilting lever system.

Dry Running Considerations

Similar to traditional white metal bearings, product lubricated bearings are not able to run dry for prolonged periods. The bearing lubrication provisions must be carefully designed to ensure continuous lubricant supply and venting must be included to eliminate the possibility of gaseous entrapment. It is usually necessary to have the flow control at the bearing exit rather than the bearing entry, as shown in Figure 7. Nevertheless, dry running can occur due to a system fault or some unforeseen pump operating condition, which may result in flashing of the process fluid. In these cases, both polymeric and ceramic bearings can withstand momentary dry running of a few seconds depending on the load, speed, and lubricating liquid. High load cases are the most critical.

In the case of the PEEK compound, the presence of PTFE and graphite in its formulation enables some degree of dry running under moderate loading conditions.

Prolonged dry running of silicon carbide bearings cause a number of material problems depending on load and temperature regime [6, 7, 8, 9]. High loads and low temperatures in the presence of water vapor cause tribochemical surface reactions that result in the formation of soft silicate films only one to three μm thicker [6]. These films "smear" and form "mud cracks" on surfaces of the silicon carbide components. Such a tribochemical film can protect the silicon carbide surface [10]. The reaction occurs because of the high localized temperature enabling the silicon carbide to oxidize with air and water vapor to form silicates (SiO and SiO_2); the greater the vapor content, the thicker the films due to the diffusion of OH^- ions through the oxidized surface. On the other hand, the wear on the silicon carbide surface for lower loads is more severe in the form of polishing and plowing of the surface. As the temperature and loads increase, the failure becomes more catastrophic as macro failure occurs.

Because of the failure modes described before, prolonged dry running will reduce the mechanical load capacity of the bearing and may indeed precipitate complete bearing failure. The least harmful dry running condition is for short periods at high load and low temperatures. Air ingestion tests carried out on silicon carbide bearings have shown that with nominal 60 percent air present, no damage was experienced under heavy load conditions (up to 6.6 MPa), which had led to failure of other types of bearings.

Effort has been ongoing to develop grades of silicon carbide with a dry lubricant phase (e.g., graphite) within the ceramic matrix. However, to date, the attendant weakening of the silicon carbide structure has precluded the use of such modified grades for highly loaded bearing applications. Some pump manufacturers have utilized the option of diamond coating silicon carbide bearing components to prolong the dry running life by a few seconds. No breakthrough in dry running capability is foreseen in the near future.

Power Consumption Under Hydrodynamic Conditions

Because the process fluids have viscosities much lower than lubricating oils, these bearings have lower power losses than oil lubricated bearings. Furthermore, the power loss for oil-lubricated ceramic bearings can be down to 20 percent of that for the same white metal bearing application, owing to the higher specific loads and oil film temperatures.

Stability

As is well known in the application of circular journal bearings, if the operating speed is sufficiently high or the bearing is lightly loaded, rotor bearing instability occurs ("oil whip" or "whirl"). This can be especially problematic in the case of vertical pumps. If properly designed, tilting pad journal bearings are inherently stable, thus avoiding such a problem.

The stiffness of a tilting pad bearing is determined by two factors: 1) the stiffness of the liquid film and 2) the stiffness of the supports. The first factor is affected by the load, speed and the viscosity; the second is mainly determined by the detail design of the bearing and support. Due to the low lubricant viscosity, product lubricated bearings suffer slightly in their stiffness and damping properties compared to oil lubricated bearings.

Damage Modes

PEEK material will display polishing and "wiping" of the surface on overload and at high temperatures. At temperatures in excess of 250°C, some pitting of the surface results due to the loss of the PTFE phase. Wiping occurs when the PEEK is severely loaded under conditions that give rise to unacceptably small hydrodynamic films. This may result in plastic deformation of the polymer in the direction of travel.

Overload of silicon carbide bearings will lead to complete destruction of the ceramic pads; there is little warning of impending failure, so steps must be taken to avoid such conditions.

Shock Loading of Silicon Carbide Bearings

Shock loading of ceramic bearings should be kept to a minimum where possible. Because of its brittle nature, silicon carbide could fail catastrophically if it were subjected to high shock loads without any damping mechanism provision. Accordingly, radial bearings are often fitted with resilient O-rings behind, and at the end of the pads, to damp any severe periodic loads (Figure 13).

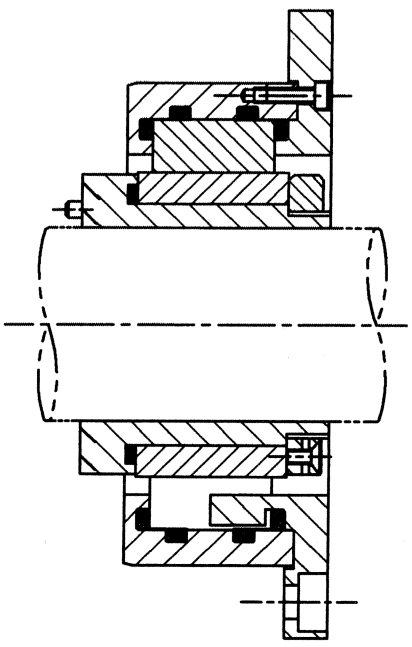

Figure 13. Silicon Carbide Radial Bearing Design for Shock Loads.

Cavitation

Ceramic bearings are also susceptible to cavitation; silicon carbides are far more sensitive to cavitation than metallic face materials [8]. Therefore, liquids with high content of free and dissolved gases could cause damage to, or failure of, silicon carbide bearings depending upon the characteristics of the pump. Failure occurs with ceramic bearings via intergranular fracture.

Unloaded Pad Instability

In low viscosity fluids, pads on radial or thrust bearings that are unloaded may become unstable with attendant "fluttering" causing premature failure of ceramic thrust pads. Some work has been carried out to eliminate this problem by tapering leading and trailing edges on each of the pads and by tightening up the clearance between the thrust collar and the pads so that the pads are, in effect, preloaded. Recent test work has confirmed the possibility of damage to unloaded thrust pads, apparently because of pad instability. PEEK pads, owing to their greater toughness will not suffer the same fate as ceramics when running in the unloaded unstable condition.

Current Range of Product Lubricated Bearing Applications

Both silicon carbide and PEEK bearings have been used in numerous demanding applications. Several examples are documented in Table 1. For example, pumps with silicon carbide bearings have operated 30,000 hours using liquid methane as a lubricant, and PEEK has been used successfully in 24,000 rpm turboexpander applications with liquefied freon lubrication.

Table 1. Examples of Product Lubricated Tilting Pad Axial and Radial Bearing Applications.

Speed (rpm)	Nom. Shaft Diam (mm)	Lubricant	Load (N)	Temperature (°C)	Bearing Type
3250	68	Sea Water	19608	4 to 30	Thrust
4200	68	Water/Crude Oil	5000	20 to 125	Thrust
1450	80	Butraldehyde	31200	-20 to 110	Thrust
3600	119	Sea Water	100000	5 to 30	Thrust
3550	50	Hydrocarbons	4450	-20 to 177	Thrust
3500	68	Demineralized Water	1000	10 to 360	Thrust
2900	46	Liquid Oxygen	1364	-180	Thrust
3600	130	Semi-lean Amine	20	-6 to 110	Journal
2900	75	Naptha	500	-55 to 100	Journal
3600	108	Hydrocarbon Condensate	20	-6 to 100	Journal
2600	40	Liquid Methane	10	-156	Journal
3600	130	Sea Water	1600	30 to 35	Journal
1450	85	Butraldehyde	2250	-20 to 110	Journal

ACTIVE MAGNETIC BEARINGS

Introduction to Active Magnetic Bearings

Basic magnetic bearing system technology has been well documented in the literature, for example O'Keefe [11]. All industrial systems include bearing actuators, position sensors located in or adjacent to the bearing cartridges, auxiliary bearings (plain bearings or rolling element bearings) in case of complete electronic failure, and the bearing controller. The bearing controller usually consists of pulse width modulated amplifiers that supply current to the bearing coils in response to shaft motion. Control algorithms, residing in analog or digital circuitry, process the shaft position signal to provide both stiffness and damping characteristics while ensuring that the shaft always is centered in the bearing stators to provide contact-free magnetic suspension.

Magnetic bearings offer the opportunity to totally eliminate the possibility of damage from dry running operation and also feature large bearing clearances to permit the passage of dirt and other contaminants through the bearing. Taken with the superior diagnostics available, these attributes provide the incentives for pump designers and end users to turn to this technology, particularly for the more demanding pump services.

The incentive to define the "safe" operating regime for fluid film bearings leads also to an interest in the limiting envelopes of operation for magnetic bearings. Magnetic bearings represent the ultimate bearing solution to the problems of mechanical bearing wear, and failure under dry running and severe overload conditions. Although magnetic bearings have lower specific load capabilities, they provide improved machine protection, because the magnetic bearing control system can immediately shut down an overloaded machine. In addition, the magnetic bearing system provides superior diagnostic information including an indication of bearing load and vibration at all times with no additional instrumentation.

Control considerations aside, a performance map for a magnetic bearing could be used in the bid evaluation process to assess the suitability of the proposed bearing for the intended service and to investigate the capability of a given magnetic bearing for off-design performance. Such a tool does not exist, in any known form, in the magnetic bearing industry. Machine builders and end users are left to sort through a confusing array of design specifications, performance data, and other technical information.

There are several variations in magnetic bearing design, but only two types have been employed in industrial applications. These two designs employ electromagnets with or without permanent magnets in their construction.

The first design has seen many applications and as a radial bearing (Figure 14) it consists of a stator component and a rotor component constructed from a stack of thin laminations of magnetically permeable material. The rotor and stator are separated by a gap through which the attractive magnetic force is developed. The stator laminations are provided in a pattern of magnetic poles, about which electrical conductors are coiled. The lamination pattern is such that a multitude of poles are formed 360 degrees around a solid circular rotor ring of the same material. In such a magnetic circuit, the flux paths are in the transverse plane only, and the design has been termed "heteropolar" since poles of alternating magnetic polarity are encountered as seen by a point on the rotor spinning past the stator poles. A typical arrangement of combined magnetic thrust and radial bearings located at the nondrive end of a pump is shown in Figure 15.

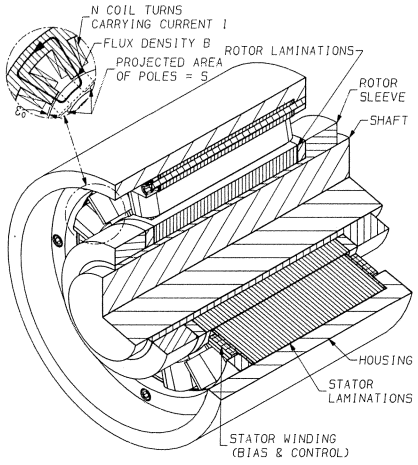

Figure 14. Heteropolar Magnetic Radial Bearing.

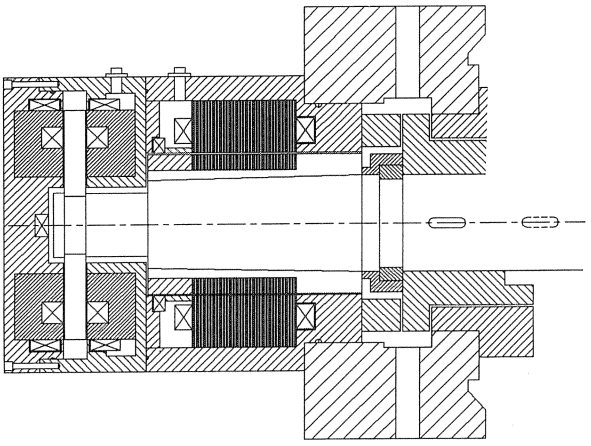

Figure 15. Typical Magnetic Radial and Axial Bearing Arrangement for Pumps.

The newer, alternative design magnetic bearing [12] also utilizes electrical coils to form an electromagnet in the transverse plane, but there are typically only four poles and these have the same magnetic polarity as seen by a point on the rotor spinning past the stator poles (Figure 16). This is the basis for the name "homopolar" given to this design. Magnetic flux from a permanent magnet located out of plane of the electromagnet travels in an axial path and, therefore, is orthogonal to the electromagnetic flux. The permanent magnet flux is used to bias the bearing and save power relative to the current bias scheme of the heteropolar design bearing. The homopolar design requires provisions to integrate the transverse and axial fluxes to produce useful energy at the gap between rotor and stator. This comprises a "lens" in the stator and a flux return sleeve on the rotor. These provisions mean that the homopolar bearing pole pieces will contain a "hetero" mixture of magnetic flux derived from both electromagnets and permanent magnets.

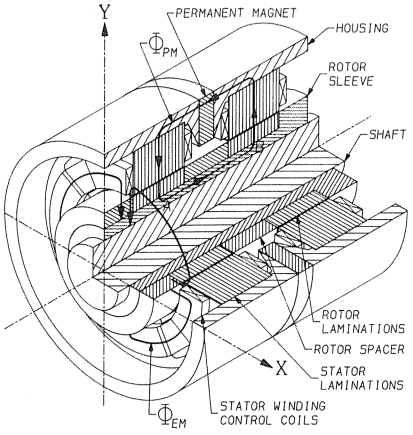

Figure 16. Homopolar Magnetic Radial Bearing.

In either design, if submersion in the pumped fluid is required, the bearing lamination stacks will be covered, or sealed, with a "can" of corrosion resistant material to protect the coils and laminations. The design of this can and selection of materials is an important element in the success of the application.

Often, one of the more important design issues with magnetic bearings is the egress of the electrical leads from the bearing stators to the outside of the bearing housings. This is easily accomplished even in the case where the bearings are submerged, since the same technology that has been applied to canned motors is relevant here. High grade, pressure rated electrical feedthroughs are readily available.

It is important to note that the heteropolar bearing design operates with opposed bearing quadrants forming a single control axis. Each quadrant needs to be driven by its own amplifier, usually in a classic H bridge configuration with the bearing coil inductance bridging the two "legs" of the H bridge. The homopolar design conserves the number of amplifiers since only one amplifier is needed to drive each control axis formed by opposed poles at each end of the bearing (A and B, Figure 16). These poles form two air gaps, each with the rotor, thereby completing the magnetic circuit.

As in the case of fluid film bearings, users of magnetic bearings are generally interested in load capacity, speed capability, and temperature capability. However, due to the unique characteristics of magnetic bearings, these parameters are not descriptive of a magnetic bearing in the same way they would be for a fluid film bearing. Rather, the related parameters of dynamic load capacity, the ratio of static load capacity to maximum load capacity, and frequency of load application are more relevant and descriptive of the bearing capability. Furthermore, these parameters can be shown to produce a limiting operating envelope not unlike that for the classic fluid film bearing.

Heteropolar Bearing Limiting Operating Envelope

The dynamic load capacity in Newtons (N) of a heteropolar bearing of given design parameters at a given frequency, f, is the minimum of:

Condition (1a):

$$\frac{\Lambda\, \Gamma^2\, A_f\, B_{sat}\, E_{pa}}{2\pi\, \mu_o\, N\, f} \tag{2}$$

Condition (1b):

$$\frac{\Lambda\, \Gamma\, A_f\, E_{pa}\, I_{pa}}{4\pi\, \varepsilon_o\, f} \tag{3}$$

Condition (2):

$$\frac{\Lambda\, \Gamma^2\, S\, B_{sat}^2}{2\, \mu_o}\,(1-K) \tag{4}$$

Condition (3):

$$\frac{\mu_o\, \Lambda\, N^2\, S\, I_{pa}^2}{8\, \varepsilon_o^2}\,(1-K) \tag{5}$$

K is the application factor of the ratio of applied static load to the maximum capacity of the bearing. The latter is dictated by the smaller of: 1) the current at which the bearing saturates, or 2) the current available from the power amplifier.

The following design parameters specify the bearing-amplifier combination: B_{sat}, N, S, ε_o, E_{pa}, and I_{pa}. The saturation induction of the magnetically permeable material chosen for bearing construction is B_{sat}. B_{sat} is generally viewed as $\leq$ 1.5 T for silicon steel and $\leq$ 2.2 T for cobalt iron. N is the number of turns of electrical conductor per pole pair of the stator. S is the projected surface area of the pole pairs in a quadrant or sector of the bearing. Quadrants are used for the basis of sizing, since the bearing acts in two quadrants along a radial axis to resist the load. ε_o is the nominal gap between rotor and stator. The control consideration of negative stiffness of an electromagnet usually restricts the rangeability of this parameter as a design variable to 0.5 to 1.0 percent of the bearing radius.

E_{pa} and I_{pa} are the pertinent amplifier specifications. E_{pa} is the maximum amplifier output voltage seen at the bearing coil connections that permits current to flow through the bearing conductors as the transistor switches open and close. I_{pa}, then, is the maximum available current rating of the power amplifier and power supply.

The other variables Λ, Γ, and A_f, are defined in the NOMENCLATURE. They represent parameters that are usually not varied by the bearing designer but are a consequence of the chosen design. The first two are loss factors that derate bearing performance from the ideal, and have been generally ignored in the development of more elementary treatments of magnetic bearing performance. The A_f factor accounts for the difference between the inductive area of the bearing and the projected area.

Equations (2), (3), (4), and (5), when plotted on log-log paper, yield a trapezoidal region (Figure 17) bounded by:

- The low frequency axis.
- Two curves that represent the maximum current slew rate limit dictated by the amplifier voltage and the bearing inductance.
- Two complete sets of families of curves for different values of the ratio of static load to maximum load, one set related to available amplifier current and the other set related to the current level at which the bearing actuator will saturate magnetically.

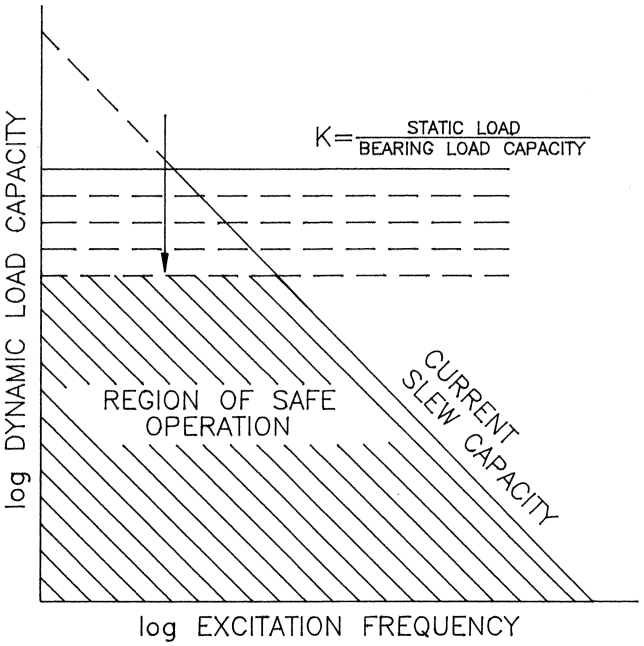

Figure 17. Limiting Operating Envelope for Magnetic Bearings.

Two sets of curves are needed for the second boundary described above to reflect the fact that magnetic bearing designers may select a design for bearing actuator saturation at levels below, equal to, or greater than levels at which the amplifier will saturate. Indeed, considering the many bearing-amplifier combinations that may be available from a given manufacturer, or in the quest to lower costs, there is some chance that amplifier saturation may occur first; a situation that normal design practice attempts to avoid.

Note that the curves for K = 0 in Figure 17, define the maximum load capacity for the bearing. This applies to either case of current limitation of the amplifier or saturation limit of the bearing actuator. Accordingly, these curves define the upper bound for bearing performance. Actual applications demanding a significant static capacity requirement will, accordingly, consume a large portion of the available dynamic capacity in meeting this static load requirement. This is reflected in the reduced dynamic load capacity as K increases. Similarly, the negatively sloped curves that reflect the slew rate limitation is lower bounded by either amplifier current limitations or bearing saturation current limitations.

It is also important to note that the trapezoidal region described above, considers theoretical bearing and amplifier performance as derated by quantifiable effects including: voltage drop to the bearing coils, fringing of the magnetic flux at the air gap, reluctance of the flux path in the rotor and stator, and magnetic flux leakage from pole to pole.

Not reflected in the Equations (2), (3), (4), and (5), is the fact that the maximum available dynamic load capacity at a given frequency will be diminished further by the amount required by the bearing system to stabilize the various natural frequencies of the rotor excited by the magnetic bearing suspension. Since the bandwidth of the magnetic bearing controller extends well above operating speed, several modes of the rotor may be excited by the magnetic bearing system. To suppress motion induced by these excitations, a portion of the available dynamic load capacity predicted by these equations is consumed. However, as a general rule, this decrement in load capacity is less than about five percent of the available capacity for good designs.

Homopolar Bearing Limiting Operating Envelope

The same design parameters used to specify the operating regime of the heteropolar bearing are used for this type of magnetic bearing also. In addition, new variables are needed to specify the permanent magnet used to bias this bearing: $B_m H_m$, the energy product of the permanent magnet material; $A_m L_m$, the volume of the magnet material; and a loss factor, υ, needed to derate the bearing from the ideal due to reluctance of the large iron paths and leakage of flux away from the bearing gap between rotor and stator. This loss factor is a complex function of magnetic circuit geometry, material properties, and flux levels, but values as large as 10 or more are possible. However, this condition does not detract from the ability to react large rotor loads with compact magnetic bearings due to advances in design and analytical tools.

The bearing dynamic capacity is the minimum of the following:

Condition (1)

$$\frac{\Lambda\Gamma^2 E_{pa} B_o}{\mu_o \pi N f}(1-K') \tag{6}$$

Condition (2)

$$\frac{2\Lambda\Gamma^2 S}{\mu_o} B_o(B_{sat}-B_o)(1-K') \tag{7}$$

Condition (3)

$$\frac{\Lambda\Gamma S N B_o I_{pa}}{\varepsilon_o}(1-K') \tag{8}$$

In the above:

$$B_o = \frac{\sqrt{\mu_o B_m H_m A_m L_m}}{\upsilon S\varepsilon_o} \tag{9}$$

i.e., the gap flux density due to the permanent magnet is proportional to the square root of the magnet material energy product, $B_m H_m$, and the magnet volume, $A_m L_m$, and is inversely proportional to the square root of the gap volume, $S\varepsilon_o$. K' in the equations for Conditions (1, 2, and 3) is defined in the APPENDIX.

Condition (1) arises from the bearing inductance. Condition (2) arises from the saturation induction of the bearing. Condition (3) arises from the possibility that the amplifier current capability will be insufficient to allow saturation of the bearing actuator.

When plotted, a trapezoidal region akin to the heteropolar bearing (Figure 17) is formed with the boundaries defined as:

- The low frequency axis.
- A curve representing the maximum current slew rate dictated by the amplifier voltage and bearing inductance.
- A family of curves for different values of the rate of static load to maximum load.

Two sets of curves are required for the third boundary defined above to reflect the fact that magnetic bearing designers may select a design for bearing actuator saturation at levels below, equal to, or greater than, levels at which the amplifier will saturate.

Use of Magnetic Bearing Limiting Operating Envelopes

Not portrayed in the limiting envelopes are controller and rotor characteristic limitations. Although the bearing-amplifier combination may be capable of providing a dynamic force output as frequency gets higher and higher, the question of the complete system loop bandwidth becomes more important. The latter can only be assessed from a macroscopic view of the entire magnetic bearing system, including the rotor. Therefore, a stability map needs to be used in conjunction with the above load *vs* frequency plot for the specific rotor system to completely specify the entire system performance. The requirement for system stability places demands on the controller frequency response that provide a separate constraint on bearing performance that is beyond the scope of this study. In the application of magnetic bearings the control of rotor natural frequencies are an important consideration and the bearing supplier must be able to provide assurances that all such resonances can be properly damped by the magnetic bearing system.

However, this consideration does not detract from the utility of the basic dynamic load *vs* frequency plot. As stated above, the plot provides a measure of the dynamic force output capability of a given bearing-amplifier combination and becomes the starting point for more detailed studies of system performance.

It would not be uncommon for pump bearings to react a static weight load and a static hydrodynamic load, in addition to synchronous unbalance. In addition, the bearings must react loads arising from vane passing frequencies. Since magnetic bearings have inherently lower specific load capacities than fluid film bearings, a pump designer may use these types of plots for considering the capability of a given bearing-amplifier combination to provide force slewing capability at synchronous frequency, while at the same time, evaluating the capability of the given bearing-amplifier combination to slew the dynamic loads arising from vane passing frequencies.

Another example of the use of this plot is to assess the capability of a given bearing-amplifier combination to react varying loads as the pump operating point changes. It is well known that pump bearing loads will increase in either direction from the best efficiency point. This plot shows the maximum available dynamic capacity at synchronous frequency, and all other frequencies of interest.

Temperature Effect

Whereas temperature has a very decided effect on fluid film bearing performance, its influence on magnetic bearing performance is more subtle. Reviewing the above design parameters for the heteropolar bearing, one finds that the only parameter directly affected is B_{sat}; the saturation induction will be mildly degraded as a function of temperature up to the Curie temperature of the material at which point the ferromagnetic effect disappears. Since this temperature is above 700°C for iron, this is not a practical limit for magnetic bearings in most pumps. If necessary, B_{sat} may be adjusted for a given bearing design to show the derating effect for high temperature operation. Also, the relative permeability, μ_r, in the Λ and Γ parameters may be similarly adjusted.

For the homopolar bearing, the energy product parameter, B_mH_m, will also need to be adjusted. In fact, many of the rare earth magnet materials are ineffective above 200°C.

Submergence Effect

In cases where the magnetic bearings are submerged directly in the pumped fluid, the fluid pressure will have a profound effect on the bearing design. The principle is illustrated in Figure 18 of a canned motor pump with canned magnetic bearings. Generally, the stator will be sealed with a "can" constructed from an engineering alloy to prevent contact of the pumped fluid with the stator windings and laminations. This can is usually unsupported over the coil slots in the stator and must be pressure rated for the full design pressure of the pump. Accordingly, the can thickness dimension is not insignificant when compared to the gap between rotor and stator. If the can material is nonmagnetic, the effective gap is greatly increased. If the can material is magnetic, short circuiting between poles will deprive the bearing gap of flux that would otherwise be used to create the attractive bearing force. Furthermore, if the can is also conductive, eddy currents will be generated that may cause overheating and ultimate failure.

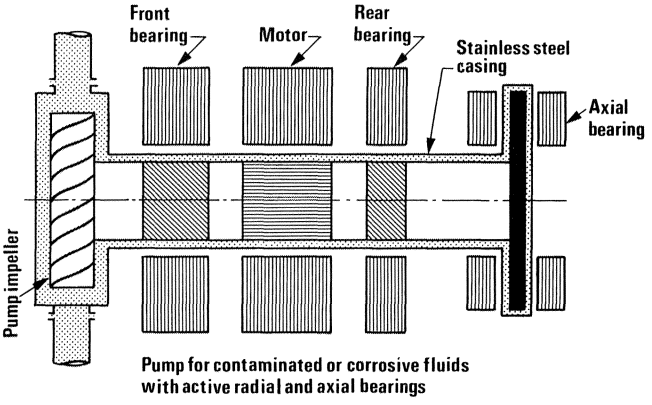

Figure 18. Principle of Canned Magnetic Bearing Construction.

Limiting Operating Envelope Examples

Depicted in Figure 19 is the limiting envelope for an uncanned magnetic radial bearing for a large 3600 rpm boiler feedpump. (E_{pa} is 300 volts, I_{pa} is 15 amps, the gap is 0.5 mm (20 mil).) A similar plot may be developed for the axial bearing. As shown in this plot, the radial bearing dynamic capacity at synchronous frequency for K = 0.3 is governed by the actuator saturation, Condition 2. On the other hand, the bearing dynamic capacity at four times running speed is limited by the amplifier power rating, $E_{pa} \times I_{pa}$, Condition 1b. The same bearing is depicted in Figure 20 canned for submergence in the boiler feedwater. In this case, with the same amplifier as above, the bearing dynamic capacity is limited to a smaller dynamic capacity due to the greater magnetic flux leakage and larger effective bearing gap created by the can, Condition 2. A net loss in dynamic load capacity of 470 N (105 lb) has resulted from canning of this bearing.

Current Range of Magnetic Bearing Applications

While the previous section describes the current operating limits in the technology of magnetic bearings for a given bearing-

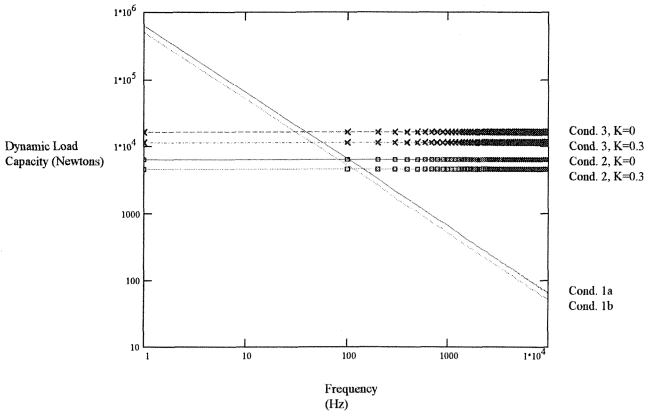

Figure 19 Typical Operating Envelope for Uncanned Heteropolar Magnetic Bearing.

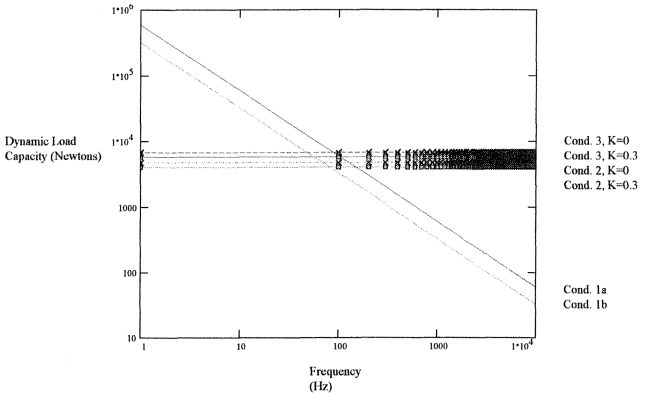

Figure 20. Typical Operating Envelope for Canned Magnetic Bearing.

amplifier combination, it is also of interest to review the total known range in various operating parameters that has been achieved in actual industrial application.

Individual bearing load capacity has exceeded 34 kN (7700 lb) on a boiler feedwater thrust bearing and 9kN (2000 lb) on a radial bearing for the same pump (Figure 21). However, there is no intrinsic reason why higher load capacities, such as those realized on compressors and turbines cannot be attained. The corresponding specific load capacity is almost 1 MPa (130 psi) on a projected area basis. 1.6 MPa (230 psi) has been achieved for similar bearings using cobalt based alloys. These figures compare to about 3.5 MPa (500 psi) for a conventional oil film bearing and mean that the many advantages of magnetic bearings come at the slight expense of larger bearings.

Speeds up to 16,000 rpm have been reported in turbopump work [13] and there are several pumps running with magnetic bearings at 3600 rpm. As discussed previously, there is no intrinsic sliding speed limit.

Environmental temperature and pressures to 175°C and 10 MPa (1500 psig) have been accommodated in a canned boiler feedwater pump. Higher temperatures are certainly feasible. A gas turbine operating on magnetic bearings at over 400°C has been achieved.

Magnetic bearings have been made immune to degradation and corrosion in environments, from boiling nitric acid to demineralized boiler feedwater, by employing a canned construction as previously discussed. A canned magnetic bearing system for a nuclear service pump complete with control cabinet is shown in Figure 22. The installation simplicity realized with a canned bearing construction of a boiler feedwater pump is illustrated in Figure 2.

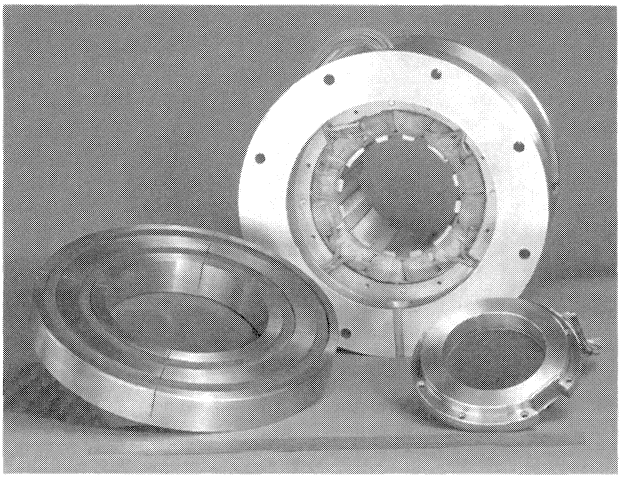

Figure 21. Magnetic Axial and Radial Bearing Examples.

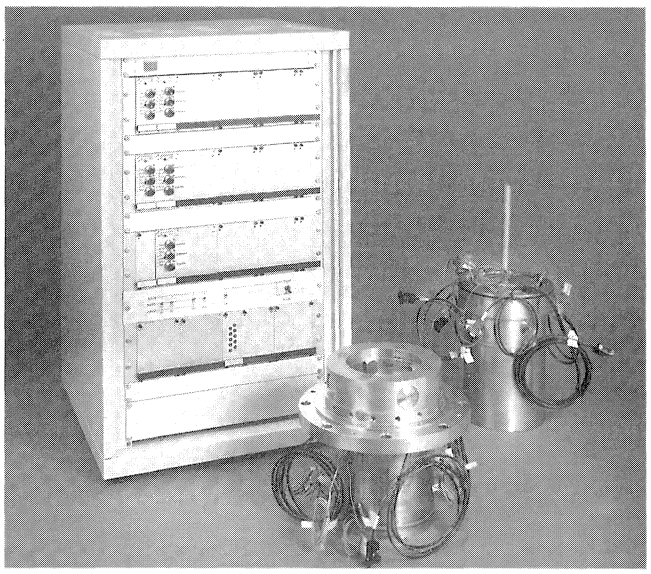

Figure 22. Canned Magnetic Bearing System for Nuclear Service.

End user familiarization with this technology will occur via training by the bearing suppliers and pump manufacturers. Proper training will allow end users to become confident in the operation and maintenance of this equipment. Operation is generally quite simple and maintenance requirements are very minimal, compared to lubrication oil systems. There are some indications that shaft vibration amplitudes are somewhat higher than comparable oil bearings, due to the lower bearing stiffness of magnetic bearings. Bearing housing vibration is generally comparable or slightly greater. However, there is no evidence that these conditions in operating magnetic bearing equipped pumps are degrading the performance of any other components, including mechanical seals.

CONCLUSIONS

Product lubricated and magnetic bearings can offer significant technical benefits and cost savings to pump manufacturers and end users. While considering the advantages of both technologies, one must be aware of the differences with oil lubricated bearing technologies and the operational constraints of these new technologies. Utilization is not just the case of bearing substitution but, rather, integrating the bearing into the pump system. In the

case of magnetic bearings, the ultimate load capacity and stability considerations must be respected. In the case of product lubrication, care must be taken to ensure that dry running is prevented. Considering all aspects of design and application, the two most successful materials to date have been PEEK thermo plastic and silicon carbide.

As discussed, PEEK thermoplastic offers high temperature product lubrication capability utilizing conventional white metal designs. It is chemically stable, able to withstand temperatures up to 250°C, and has found a significant market in high temperature bore hole pump applications. Silicon carbide bearings have extremely high resistance to impurities (including hard particles), can operate between −200°C and 380°C, have high load capacities, and can be lubricated by almost any liquid such as crude oil, acids, or liquefied gas.

Magnetic bearings allow even more advanced pump designs with no worry about possible dry running or contaminant damage. Good load and structural resonance information is required to avoid overloads and ensure system stability. Proper integration into pump design allows unequalled diagnostic information for health monitoring and preventative maintenance of other pump mechanical components.

Surveys report that up to 90 percent of reported pump failures are due to either mechanical seal or bearing problems. Therefore, with the advantages of these new bearing technologies, including the elimination of many of the mechanical seals, these bearings offer a route to reducing downtime and increasing reliability. Compliance with environmental and safety regulations will also be aided by the use of such bearings. The choice of the proper bearing technology, product lubricated or magnetic, will depend upon the unique requirements for each application.

The main opportunities for these technologies will be in the sealless pump market because of economic, legislative, and environmental pressures. Development still continues by both the pump and bearing companies to achieve advanced pump designs.

APPENDIX

Using a similar approach as Bornstein [14], the net dynamic force available from an opposed pair of magnets is:

Equation (A-1):

$$F_{net} = \frac{2S}{\mu_o} B_o \Delta B \tag{10}$$

Where B_o is the constant bias flux density in the gap between rotor and stator and ΔB is the perturbation flux density.

Heteropolar Bearing

The bias flux in a heteropolar bearing is obtained from a bias current. For best performance, this current should be one-half of the maximum available, $I_{sat}/2$ (or $I_{pa}/2$ if $I_{pa} < I_{sat}$), in order to provide equal perturbation fluxes, positive and negative, from the bias point of both top and bottom magnets.

Including the reluctance of the magnet flux path that detracts from the ideal force available, the flux density due to current excitation is:

Equation (A-2):

$$B = \frac{\mu_o NI}{2\varepsilon_o + l_i/\mu_r} \tag{11}$$

Substituting Equation (A-2) into Equation (A-1) and considering a factor Λ to account for iron reluctance and flux leakage leaves:

Equation (A-3):

$$F_{net} = \Lambda \left[\frac{\mu_o N^2 S}{2\varepsilon_o^2} \right] I_b \Delta I \tag{12}$$

where:

$$\Lambda = \frac{\lambda}{\left(1 + \dfrac{l_i}{2\mu_r \varepsilon_o}\right)^2} \tag{13}$$

ΔI, the perturbation current is made up of two parts ΔI_o and ΔI_{dyn} (sinusoidal). ΔI_o is a static perturbation current to react the static loads, F_s, including weight,

$$\Delta I_o = \frac{2\varepsilon_o^2 F_s}{\Lambda \mu_o N^2 S I_b} \tag{14}$$

and:

$$\Delta I_{dyn} = MIN \begin{bmatrix} \dfrac{E}{\omega L} \\ I_{pa} - (I_b + \Delta I_o) \\ I_{sat} - (I_b + \Delta I_o) \\ I_{pa}/2 - \Delta I_o \\ I_{sat}/2 - \Delta I_o \end{bmatrix} \tag{15}$$

Note that:

$$L = \frac{\mu_o N^2 S}{2A_f \varepsilon_o \Gamma} \tag{16}$$

and $A_f = 1.8$ for a radial bearing; 2.0 for an axial bearing.

Defining $K = F_s/F_{max}$ where F_{max} is the maximum load capacity available then $F_{dyn} = F_{net} - F_s$ and substituting ΔI_{dyn} into (A-3) yields four unique dynamic load capacity restrictions corresponding to the dynamic perturbation currents.

Condition (A-1a):

$$\Delta I_{dyn} = \frac{A_f \varepsilon_o \Gamma E_{pa}}{\mu_o \pi N^2 S f} \qquad F_{dyn} = \frac{\Lambda \Gamma^2 A_f B_{sat} E_{pa}}{2 \pi \mu_o N f} \tag{17}$$

Condition (A-1b):

$$\Delta I_{dyn} = \frac{A_f \varepsilon_o \Gamma E_{pa}}{\mu_o \pi N^2 S f} \qquad F_{dyn} = \frac{\Lambda \Gamma A_f E_{pa} I_{pa}}{4 \pi \varepsilon_o f} \tag{18}$$

Condition (A-2):

$$\Delta I_{dyn} = \frac{I_{pa}(1-K)}{2} \qquad F_{dyn} = \frac{\Lambda \mu_o N^2 S I_{pa}^2}{8 \varepsilon_o^2} (1\text{-}K) \tag{19}$$

Condition (A-3):

$$\Delta I_{dyn} = \frac{\Gamma \varepsilon_o B_{sat}}{\mu_o N} (1\text{-}K) \qquad F_{dyn} = \frac{\Lambda \Gamma^2 S B_{sat}^2}{2\mu_o} (1\text{-}K) \tag{20}$$

B_{sat}, the saturation flux density, is illustrated in the normal magnetization curve and hysteresis loop of Figure A-1.

Homopolar Bearing

Following Reistad [15], the magnetic flux density at the gap of a permanent magnet circuit is:

Equation (A-4)

$$B_g = \sqrt{\frac{\mu_o B_m H_m A_m L_m}{\upsilon S \varepsilon_o}} \tag{21}$$

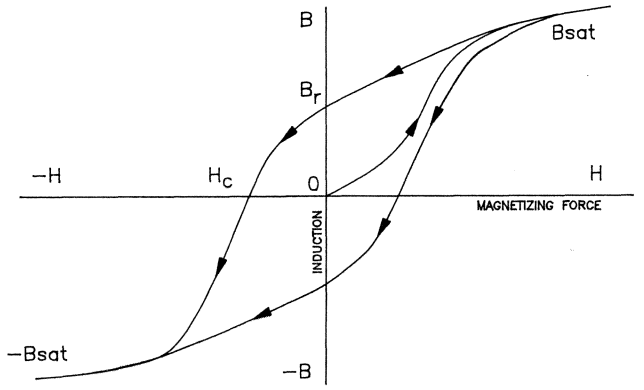

Figure A-1. Normal Magnetization Curve and Hysteresis Loop.

where $\upsilon = \sigma_l R_f$, the overall circuit loss factor. $B_m H_m$, the magnet energy product; and $A_m L_m$ the magnet volume. The magnet energy product is illustrated in the magnetization and energy product curves of Figure A-2.

Substituting B_g from (A-4) above for B_o and ΔB_o from (A-2) into Equation (A-1) above yields,

$$F_{net} = \frac{\Lambda \Gamma S N}{\varepsilon_o} \sqrt{\frac{\mu_o B_m H_m A_m L_m}{\upsilon S \varepsilon_o}}\, \Delta I \qquad (22)$$

Now,

$$F_{dyn} = F_{net} - F_s$$

Equation (A-5)

$$F_{dyn} = \frac{\Lambda \Gamma S N}{\varepsilon_o} \sqrt{\frac{\mu_o B_m H_m A_m L_m}{\upsilon S \varepsilon_o}}\, \Delta I_{dyn} (1-K') \qquad (23)$$

and:

Equation (A-6)

$$\Delta I_{dyn} = MIN \left[\frac{E}{\omega L} \; ; \; I_{pa} \; ; \; I_{sat} \right] \qquad (24)$$

Noting that $A_f = 1$ for a homopolar bearing in the inductance equation and substituting I_{dyn} for the three conditions from (A-6) into (A-5) yields three unique dynamic load capacity restrictions corresponding to the three unique dynamic perturbation currents,

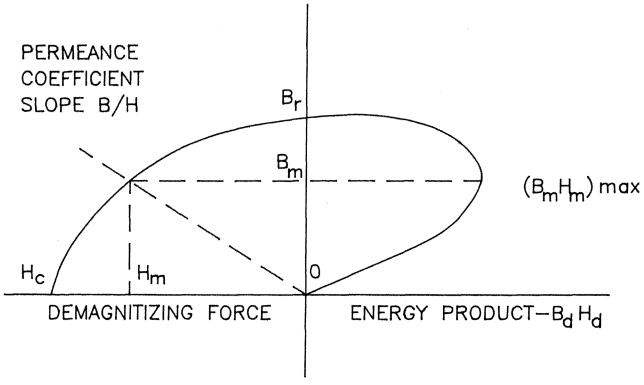

Figure A-2. Magnetization and Energy Product Curves.

Condition (A-1):

$$\Delta I_{dyn} = \frac{E_{pa} \varepsilon_o \Gamma}{\mu_o \pi N^2 S f}$$

$$F_{dyn} = \frac{\Lambda \Gamma^2 E_{pa} B_o}{\mu_o \pi N f} (1-K') \qquad (25)$$

Condition (A-2):

$$\Delta I_{dyn} = I_{sat} \qquad (26)$$

$$F_{dyn} = \frac{2\Lambda \Gamma^2 S}{\mu_o} B_o (B_{sat} - B_o) (1-K') \qquad (27)$$

Condition (A-3):

$$\Delta I_{dyn} = I_{pa} \qquad (28)$$

$$F_{dyn} = \frac{\Lambda \Gamma S N I_{pa} B_o}{\varepsilon_o} (1-K') \qquad (29)$$

In these cases, K' represents the ratio of static load carried by current only to the maximum load capacity.

NOMENCLATURE

A_f Ratio of projected bearing area to inductive bearing area (−)
A_m Permanent magnet area (m^2)
b Pad breadth (m)
B_g Gap flux density
B_m Permanent magnet flux density (Tesla)
B_o Bias flux density (Tesla)
B_{sat} Saturation flux density (Tesla)
C Empirical constant in film thickness equation (−)
E_{pa} Maximum available amplifier voltage (volt)
F Force (N)
f Excitation frequency (Hz)
F_{dyn} Dynamic force (sinusoidal) (N)
F_s Static force (N)
F_{net} Net force from opposed magnets (N)
h_{min} Minimum fluid film thickness (m)
H_m Permanent magnet field strength (Oersted)
I Current (amps)
I_b Bias current (amps)
I_{dyn} Dynamic current (sinusoidal) (amps)
l_i Mean flux path length in magnet iron circuit (m)
l_m Permanent magnet length (m)
I_{pa} Maximum amplifier current (amps)
I_{sat} Current at which bearing saturates (amps)
K Ratio of static force to maximum load capacity (−)
L Bearing inductance (Henrys)
N Turns per pole pair (−)
R_f Reluctance factor accounting for magnetomotive force drop in magnet iron circuit (−)
S Projected area of magnetic pole pairs after including lamination packing factor (m^2)
U Sliding speed (m/s)
W_p Load per pad (N)

Greek Letters

Γ Reluctance variable group (−)

$$\Gamma = \frac{2\varepsilon_o + l_i/\mu_r}{2\varepsilon_o} \qquad (30)$$

ε_o Gap length between rotor and stator (m)
η_e Pad effective viscosity (N−s/m^2)
Λ Variable group accounting for flux leakage and reluctance of iron in magnetic circuit (−)

$$\Lambda = \frac{\lambda}{\left(1 + \frac{l_i}{2\mu_r \varepsilon_o}\right)^2} \qquad (31)$$

λ Loss factor for leakage of magnet flux at air gap (−)
μ_o Permeability of free space = $4\pi \times 10^{-7}$ (Henry/m)
μ_r Relative permeability (= μ/μ_o) (−)
σ_l Loss factor for leakage of magnet flux away from gap (−)
υ Loss factor including reluctance in magnet iron circuit and leakage flux away from gap (=$R_f\sigma_l$) (−)

REFERENCES

1. Leopard, A. J., "Tilting Pad Bearings–Limits of Operation," ASLE 30th Annual Meeting, Atlanta, Georgia (1975).
2. Smith, H., "Is the Writing on the Wall for Oil Lubricated Bearings in Pumps?" World Pumps (1995).
3. Marscher, W. D., and Jen, C. W., "Development of an Active Magnetic Bearing for a 50 HP Canned Motor Pump," ROMAG 91 Magnetic Bearing Conference, Washington D.C. (1991).
4. Martin, F. A., "Tilting Pad Thrust Bearings: Rapid Design Aids," (1970).
5. Leopard, A. J., "Principles of Fluid Film Bearing Design and Application," *Proceedings of the Sixth Turbomachinery Symposium*, Turbomachinery Laboratory, Texas A&M University, College Station, Texas, pp. 207-230 (1977).
6. Dong, X., et al, "Wear Transition Diagram for Silicon Carbide," Tribology International, *28* (1995).
7. Blomberg, A., et al, "An Electron Microscopy Study of Worn Ceramic Surfaces," Tribology International (1993).
8. Crammer, D. C., "Friction and Wear Properties of Monolithic Silicon-Based Ceramics," Bendix Technology Center (1984).
9. Blouin, A. and Frenc, J., "Experimental Study to Analyze the Tribological Behavior of Silicon Carbide in Water," Leeds/Lyon Tribology Symposium, Leeds, United Kingdom (1992).
10. Klafte, D., "Fretting Wear of Ceramics," Tribology International (1989).
11. O'Keefe, W., "Consider the Magnetic Bearing, Practically Here for Pumps," Power Magazine (March 1993).
12. Meeks, C., "Development of a Compact Light Weight Magnetic Bearing," 35th ASME International Gas Turbine Congress and Exhibition, Brussels, Belgium (1990).
13. Hawkins, L. A. and Scharrer, J. K., "Development of Rotordynamic Simulator for Rocket Engine Turbopump with Magnetic Bearings" (1994).
14. Bornstein, K. R., "Dynamic Load Capabilities of Active Magnetic Bearings," ASME 90-Trib-50 (1990).
15. Reistad, K., et al, "Magnetic Suspension for Rotating Equipment," Project Final Report, Phase I, National Science Foundation (1980).